Journal Pre-proofs

Thermally reactive *N*-(2-hydroxypropyl)methacrylamide (HPMA) amphiphiles for drug solubilisation

Ali Alsuraifi, Essyrose Mathew, Dimitrios A. Lamprou, Anthony Curtis, Clare Hoskins

PII: S0378-5173(21)00375-6
DOI: https://doi.org/10.1016/j.ijpharm.2021.120570
Reference: IJP 120570

To appear in: *International Journal of Pharmaceutics*

Received Date: 6 October 2020
Revised Date: 10 March 2021
Accepted Date: 31 March 2021

Please cite this article as: A. Alsuraifi, E. Mathew, D.A. Lamprou, A. Curtis, C. Hoskins, Thermally reactive *N*-(2-hydroxypropyl)methacrylamide (HPMA) amphiphiles for drug solubilisation, *International Journal of Pharmaceutics* (2021), doi: https://doi.org/10.1016/j.ijpharm.2021.120570

Thermally reactive *N*-(2-hydroxypropyl)methacrylamide (HPMA) amphiphiles for drug solubilisation

Ali Alsuraifi[1,2], Essyrose Mathew[3], Dimitrios A. Lamprou[3], Anthony Curtis[1], Clare Hoskins[1,4*]

1 School of Pharmacy and Bioengineering, Keele University, Keele, ST5 5BG, UK
2 College of Dentistry, University of Basrah, Basrah, 61004, Iraq
3 School of Pharmacy, Queen's University Belfast, Belfast, BT9 7BL, UK
4 Department of Pure and Applied Chemistry, University of Strathclyde, Glasgow, G1 1RD, UK

*Corresponding author: Dr Clare Hoskins, clare.hoskins@strath.ac.uk

Abstract: Thermally active polymers, can respond structurally to temperature changes, making them interesting as potential drug delivery vehicles. Polymers of *N*-(3-aminopropyl) methacrylamide hydrochloride (APMA) are cationic with primary amine groups in their structure, which have been explored in biomedical applications via post-polymerisation modifications. In this work, we synthesised amphiphilic APMA monomers using hydrophobic pendant groups via conjugation onto their primary amine group. The pendant groups chosen in this study were palmitoyl, dansyl and cholesteryl moieties. The amphiphilic monomers were subsequently copolymerized with *N*-(2-hydroxypropyl)methacrylamide (HPMA) using varied monomer feed ratios resulting in a thermo-responsive system. The ability of the resultant aggregates in aqueous solution to encapsulate and liberate model drugs (e.g., propofol, griseofulvin and prednisolone) was then determined. Our data showed that the HPMA based formulations were capable of loading the model drug molecules inside their lipophilic core; HPMA-co-(APMA-Dansyl 2%) exhibited the largest drug encapsulation ability. Subsequently, poly(ethylene glycol) (PEG) was incorporated into the intrinsic polymer structure. This resulted in a more rapid drug release profile, whereby 100% of griseofulvin and prednisolone were liberated after only 4 h, which was only 5% and 10% before the PEG inclusion, respectively. Similarly, propofol showed 70% liberation from the polymer aggregate after 24 h, compared with only 30% liberation pre-PEGylation. These studies give an insight into the potential of the HMPA based amphiphiles as thermally responsive cargo carrier/release systems which could be exploited in the delivery of poorly soluble drugs.

Keywords: Thermo-responsive polymers, drug delivery, intelligent nanomedicine, smart polymers, drug solubilisation

1. Introduction

Thermally active polymers have attracted great attention for their potential in the area of drug delivery. They are classed by their lower critical solution temperature (LCST) or upper critical solution temperature (UCST) properties. Relevant specifically for drug delivery, those polymers that exhibit structural changes or deformation at their LCST are of interest. These structural changes lead to the ability to change polymer solubility in aqueous environments [1]. Such deformation could help to overcome the challenges faced currently in the delivery of compounds to site of need, such as in cancer chemotherapy where highly potent compounds cause great physiological detriment when circulated systemically, often hindering their dose threshold and use.

Some of the most successful thermally active polymeric drug delivery systems are based on the use of poly(*N*-(2-hydroxypropyl) methacrylamide) (HPMA) polymers and their derivatives [2-7]. HPMA is non-immunogenic, biocompatible, allows the possibility of functionalization and acts in a thermo-responsive manner [3]. *N*-(3-aminopropyl)methacrylamide (APMA) is a monomer, which possesses a primary amine group in its structure. In the literature, APMA is reported in the fabrication of polymers and their associated nano-aggregates, which have been used in for the delivery of drug compounds and genes [8]. APMA is easily tailored for applications via modification of the primary amine residue in its structure, enabling the possible conjugation of a host of hydrophobic groups. Chu and colleagues reported the grafting of an HPMA-co-APMA polymer with a BM9 peptide [9]. The resultant copolymer formula was used for solubilisation and controlled release of bivalirudin in the treatment of spinal cord injury. The data showed decreased proliferation and reduced gliosis in rat models after treatment with the bivalirudin-release depots [9].

This work reports a series of APMA-HPMA based thermally active polymers, which offer ease of synthesis and control over physicochemical properties using hydrophobic pendant groups that have previously shown to be beneficial in nano-based drug solubilisers [10-13]. The benefits of this system over existing thermally responsive systems is the ease of design, based on proposed use and synthesis. In order for such delivery systems to possess potential for commercial scale-up, simple synthetic routes are preferred, such as the one reported here. The APMA-HPMA copolymers were fabricated using modified APMA monomers bearing hydrophobic palmitoyl, dansyl and cholesteryl moieties. The hydrophobic moieties were conjugated onto the APMA primary amine residue, the monomer derivatives were then polymerized with water soluble HPMA monomers, and subsequently poly(ethylene glycol) (PEG) was incorporated into the polymer structure via block copolymerisation. Such polymers were capable of nano-aggregate formation in aqueous solutions, which could be explored for drug delivery.

Poly(allylamine) graft polymers modified with palmitoyl, cholesterol and dansyl moieties have been explored previously with interesting accounts of the ability to load drugs into their nano-aggregates [10-13]. They have been reported as universal drug solubilisers due to their ability to encapsulate four model drugs of differing molecular weights and stereo-chemistries (e.g., propofol, griseofulvin, prednisolone, and Bisnaphthalimidopropyldiaaminooctane (BNIPDaoct)) [11-13]. Cholesterol has also been shown to regulate structural integrity factors such as membrane permeability, which influences trafficking [14]. Zheng and colleagues reported that hydrophobic cholesterol derivatives, such as the cholesteryl residues used in this study, are capable of enhancement in drug loading levels in alginate-based delivery systems [15].

For this work, the ability of the series of HPMA-APMA derivatives to encapsulate and solubilise three commonly used model lipophilic drug compounds (e.g., propofol, griseofulvin and prednisolone) was explored. Each drug is used clinically, but their poor physicochemical properties require formulation before use. These drugs, were chosen not only for their lipophilicity but also due to their differing molecular weights and architectures, in order to determine whether the molecular structure or size of the drug affected incorporation into the polymers; more specifically, were chosen to investigate whether the polymers could be used as drug solubilisers for a range of compounds of different molecular weight and stereo-chemistries. Here, we report the ability of the HMPA-APMA amphiphiles created to incorporate drug into their self-assemblies and evaluate their ability to release drugs in a thermo-responsive manner (Figure 1).

2. Materials and Methods

N-(2-hydroxypropyl) methacrylamide and *N*-(3-aminopropyl) methacrylamide hydrochloride, ≥ 98% were purchased from Polysciences, Inc, USA. Deuterated chloroform-D (D, 99.98%), and deuterated methanol-D_4 (D, 99.98%) were purchased from Cambridge isotope laboratories, Inc., UK, deuterated dimethyl sulfoxide-D_6 (D, min. 99.8%) was purchased from Apollo Scientific Ltd., UK. Propofol, griseofulvin and prednisolone were purchased from Sigma Aldrich, UK. Syringe filters were purchased from Fisher Scientific, UK. All other chemicals were purchased from Alfa Aesar, UK and solvents from VWR, UK.

2.1 Hydrophobic Modification of APMA monomers

In a round bottom flask (RBF), APMA (1.79 g, 10 mmol) with 10 mmol of palmitoyl chloride, dansyl chloride or cholesteryl chloroformate was mixed with anhydrous dimethylformamide (DMF, 50 mL), followed by continuous stirring under argon atmosphere at 0°C. Subsequently, triethylamine (2.92 mL, 21 mmol) was added dropwise to the mixture. The reaction mixture was stirred at 0 °C for 3 h and was monitored by TLC. The DMF was removed and the solid residue was dissolved in dichloromethane (DCM). Water was used to extract any remaining triethylamine hydrochloride. The solvent was removed forming a white solid (palmitoyl-APMA, P-APMA), a yellow liquid (dansyl-APMA, D-APMA) and a white solid (cholesteryl-APMA, C-APMA), respectively (Figure 2). Characterisation of the final products was determined by measuring the melting point using an Advanced Digital Melting Point instrument SMP3 (Bibby Sterilin Ltd, UK), Fourier transform infrared spectroscopy using a Nicolet iS10 FT-IR (Thermo scientific Ltd, USA) and nuclear magnetic spectroscopy (300 MHz Bruker Avance 300).

2.2 Polymerization of HPMA with APMA derivatives

HPMA copolymerization with the APMA derivatives was carried out at 60 °C in methanol with azobisisobutyronitrile (AIBN) as the initiator [16]. HPMA and APMA derivates were placed inside an ampule connected to a Schlenk line. The oxygen was removed in three vacuum-nitrogen aspiration cycles, before degassed methanol (5 mL) and a solution of AIBN (0.55 mg) in 1 mL methanol was added at varied ratios (Table 1). Polymerization was achieved over a 24 h period at 60 °C inside the sealed ampule. Product was obtained by precipitation in acetone before purification in methanol, which was repeated three times. Polymers were characterised using Fourier transform infrared (FTIR) spectroscopy using a Nicolet iS10 FT-IR (Thermo scientific Ltd, USA) and nuclear magnetic resonance (NMR) spectroscopy (300 MHz Bruker Avance 300).

2.3 Synthesis of PEGylated block copolymer

Synthesis of the diblock copolymer of (HPMA-co-APMA-R)-b-PEG (Figure 3) proceeded in

methanol with a radical initiator. A glass tube was filled with 20:80 PEG: HPMA-co-APMA-R molar ratios respectively, followed by AIBN initiator under a nitrogen atmosphere. The reaction proceeded for 24 h at 60 °C with continuous stirring. After which, the block copolymers were precipitated in methanol. Polymers were characterised using FT-IR (Thermo scientific Ltd, USA) and NMR (300 MHz Bruker Avance 300).

2.4 Nuclear Magnetic Resonance (NMR) Spectrometry

Polymers were dissolved in $CDCl_3$ and data for their proton (^1H) and carbon (^{13}C) spectra were collected on a Bruker Avance instrument at a frequency of 300 MHz at 25 °C.

2.5 Fourier Transform Infrared (FTIR) Spectroscopy

Polymers or formulations were freeze-dried and scanned (64 scans) on a Nicolet iS10 FT-IR (Thermo scientific Ltd, USA) with an ATR attachment. Scans were collected after background correction.

2.6 Differential Scanning Calorimetry (DSC)

The polymers were analysed using a Netzsch 214 Polyma (Germany) differential scanning calorimeter (DSC). Samples placed in an aluminium pan and sealed with an aluminium lid. The samples were then subject to heating at a rate of 10°C/min from 30°C to 150°C with a continuous purge of nitrogen gas at 40 ml min^{-1}. The heat flow (mW) as a function of temperature was recorded for each sample.

2.7 Thermogravimetric Analysis (TGA)

The thermal degradation properties of the polymers were analysed using Q500 Thermogravimetric analysis (TA instruments, Bellingham, WA). Samples heated from 20°C to 500°C at a heating rate of 10°C/min under nitrogen flow at a rate of 40 ml min^{-1}.

2.8 Drug Loading

Various polymer concentrations (e.g., 1, 3, and 6 $mgmL^{-1}$) diluted in deionised water were solubilised using a probe sonicator (Soniprep 150 plus, MSN, UK) with sonication for 10 min before leaving solutions to cool to room temperature. Hydrophobic drugs were added to the cooled solutions at 1:1, 1:5 and 1:10 initial polymer: drug weight ratio. The mixtures were further sonicated for 10 min and allowed to cool to room temperature. The solutions were then passed through a 0.45 μm syringe filter (with pre-filters) in order to remove any unencapsulated drug [11,13]. Formulations were characterised using photon correlation spectroscopy and zeta potential measurement. Samples were stored at 5±1 °C prior to analysis. The amount of drug incorporation was determined as below:

2.8.1 Quantification of Propofol

Propofol quantification was determined using reverse-phase high-performance liquid chromatography (HPLC) coupled to an ultraviolet–visible (UV) detector (Perkin Elmer Flexar LC, Netherlands). Samples were passed through a Pinnacle DB C18 5 μm x 150 mm x 3.2 mm column (Restek, UK) at 25 °C. The mobile phase was made up using methanol:water (80:20 v/v), flow rate: 1.0 $mLmin^{-1}$ and detection at 229 nm, with a retention time of approximately 2.2 min [11]. Sample concentration was determined using a calibration curve in mobile phase, R^2= 0.998. All samples were run in triplicate, average sizes and standard deviations calculated in Microsoft Excel.

2.8.2 Quantification of Griseofulvin

Griseofulvin quantification was measured using reverse phase HPLC coupled to a UV detector

(Perkin Elmer Flexar, US). Samples were passed through a Pinnacle DB C18 5 µm x 150 mm x 3.2 mm column (Restek, UK) at 25 °C. The mobile phase was made up using 45:55 v/v of acetonitrile:45 mM potassium dihydrogen phosphate in water, pH adjusted to 3 using orthophosphoric acid, flow rate:1 $mLmin^{-1}$ and detection at 293 nm, with a retention time of 2.8 min [11]. Sample concentration was determined using a calibration curve in mobile phase, $R^2 = 0.999$. All samples were run in triplicate, average sizes and standard deviations calculated in Microsoft Excel.

2.8.3 Quantification of Prednisolone

Prednisolone quantification was measured using reverse phase HPLC coupled to a UV detector (Perkin Elmer Flexar, US). Samples were passed through a Pinnacle DB C18 5 µm x 150 mm x 3.2 mm column (Restek, UK) at 25 °C.. The mobile phase made up using 64:36 (v/v) water:acetonitrile, flow rate: 1 $mLmin^{-1}$, detection at 243 nm, and retention time approximately 1.65 min [11]. Sample concentration was determined using a calibration curve in mobile phase mobile phase, $R^2 = 0.999$. All samples were run in triplicate, average sizes and standard deviations calculated in Microsoft Excel.

2.9 Photon correlation spectroscopy and zeta potential measurement.

Polymer aggregates and formulations were suspended in water and aliquoted into folded capillary cells. The particle size and zeta potential measurements were determined at 25 °C using a Malvern ZS Zetasizer (Malvern, UK). Samples were run in triplicate and standard deviations recorded.

2.10 *In vitro* drug release

Drug release was determined at set time points at varied temperature and pH. The formulations (2 mL) were pipetted into a visking membrane with molecular weight cut off = 12-14 kDa. The tube was then dialyzed exhaustively against deionised water (200 mL, pH 7) with stirring over 24 h at varied temperature (e.g., 5 °C, 30 °C, 40 °C, 50 °C). At set time points, 1 mL of the exterior deionised water solution was aliquoted and replaced to ensure sink conditions. The percentage of drug release was measured using HPLC and was calculated using the starting weight and weight of drug detected in the exterior dialysis solution [11,13]. All samples were run in triplicate, average sizes and standard deviations calculated in Microsoft Excel.

3. Results

3.1 Characterisation of Modified AMPA monomers

The modified monomers were successfully synthesised, with their physical properties shown in Table 2. Chemical analysis was carried out using NMR (SI-Figure 1). The ^{1}H NMR spectrum of AMPA-P (SI-Figure 1A) showed peaks that are indicative of the presence of the palmitoyl groups. Similarly, the other peaks observed can be attributed to presence of the AMPA residues. The ^{13}C-NMR spectrum (SI-Figure 2A) also confirmed this. FTIR spectroscopy (SI-Figure 3A) agreed with the observations of the NMR study, whereby a peak at 3294 cm^{-1} was observed, which was due to -NH stretching vibrations within the APMA whilst at 2916 cm^{-1} the sharp band observed was due to C-H stretching, and the peak at 1637 cm^{-1} can be attributed to the amide carbonyl group.

The AMPA-D FTIR spectrum (SI-Figure 3B) indicated that the dansyl modification had been successful. Here a broad band was observed at 3289 cm^{-1} due to of N-H presence and could be due to the sulphonyl residue. The peak at 1655 cm^{-1} can be attributed to the amide C=O group

and other peaks (at 1600-1400 cm^{-1}) are attributed to an aromatic residue, confirmed the dansyl coupling onto the APMA. The ^{1}H and ^{13}C NMR spectra (SI-Figure 1B&2B) of compound APMA-D was in agreement with the FTIR. Here, peaks were observed that could be attributed to the aromatic dansyl moiety as well as the APMA residue, in common with the spectra for APMA-P.

For AMPA-C, as expected the ^{1}H NMR spectrum (SI-Figure 1C) highlighted the presence of the alkyl protons in the cholesteryl pendant, as well as the APMA protons. The ^{13}C-NMR spectrum (SI-Figure 2C) also reflected the saturated nature of the cholesteryl group. The FTIR spectrum (SI-Figure 3C) further confirmed cholesteryl attachment with the presence of the two peaks at 3386 cm^{-1} and 3272 cm^{-1}, which correspond to the N-H group. The observed peaks at 1702 cm^{-1} and 1659 cm^{-1} correspond to the urethane C=O and amide C=O, respectively.

3.2 Characterisation of polymerisation of HPMA and APMA monomers

The FTIR and NMR spectra for polymerised HMPA-AMPAs are shown in SI-Figure 4 and Figure 4, respectively. A broad band (3351 cm^{-1}) with two overlapping peaks was observed in the FTIR spectra for poly(HPMA-co-APMA-P) (SI-Figure 4A) indicating the presence of the O-H groups from the HPMA. Peaks characteristic of C=O groups in such polymers were observed at 1653 cm^{-1} and 1615 cm^{-1}. As illustrated by the ^{1}H-NMR spectrum of poly(HPMA-co-APMA-P) (Figure 4A) peaks were observed which indicated the presence of the polymer backbone as well as the aliphatic palmitoyl pendant.

FTIR of the HPMA-co-APMA-D polymer (SI-Figure 4B) showed a band at 3299 cm^{-1} which was due to the O-H peak overlapped with the N-H group peak. Peaks characteristic of C=O groups in such polymers were observed at 1653 cm^{-1} and 1615 cm^{-1}, whilst further peaks between 1550-1300 cm^{-1} were due to aromatic moieties in the dansyl pendant. ^{1}H NMR spectroscopy (Figure 4B) of the poly(HPMA-co-APMA-D) showed a similar profile to the poly(HPMA-co-APMA-P), also obvious from this spectrum was the presence of the protons attributed to the aromatic dansyl group.

The FTIR spectra for the HMPA-co-APMA-C, seen in SI-Figure 4C, showed a band at 3299 cm^{-1} which was due to a peak for the O-H groups overlapping with one for the N-H groups. As before, peaks characteristic of C=O groups in such polymers were observed at 1653 cm^{-1} and 1615 cm^{-1}. The ^{1}H NMR spectrum for poly(HPMA-co-APMA-C) (Figure 4C) was in agreement with other spectra which showed the presence of the polymer backbone, and also for the saturated cholesteryl group, thus confirming successful polymerisation.

The DSC graphs for the polymerised HMPA-AMPAs are shown in Figure 5. The melt peaks (Tm) for poly(HPMA-co-APMA-P), HPMA-co-APMA-D and HMPA-co-APMA-C are 55.3°C, 56.7°C and 70.7°C, respectively. A second peak is also visible in these formulations; this may be due to thermal decomposition of the formulation within the temperature range of 100°C to 130°C.

As seen in SI-Figure 6 the TGA, thermograms showed a rapid degradation between 281.89°C and 466.51°C for HMPA-co-APMA-C (A). Degradation occurred between 299.65°C and 495.74°C in poly(HPMA-co-APMA-P (B). In both of these polymers a slight degradation of around 12% occurring between ambient temperature and 280°C, prior to onset of rapid degradation. HPMA-co-APMA-D (C) showed a slow degradation over a range of temperatures with degradation beginning around 58.68°C and ending around 469.34°C.

3.3 Characterisation of PEGylated block copolymers

The FTIR spectra of poly(HPMA-co-APMA-D)-b-PEG (SI-Figure 5) showed a broad band at 3299 cm^{-1} with two peaks, as observed in the non-PEGylated polymer, which was due to overlapping OH and NH peaks. However, confirmation that block copolymerization with the PEG could be deduced due to the notable increase in the peak size (transmission), as PEG is largely visible in this region. The ^{1}H NMR spectrum (Figure 4D) showed the presence of the polymer backbone, however, protons attributed to the PEG group overlapped these significantly. The presence of the dansyl protons were observed in the expected region of the spectrum.

The Tm for the poly(HPMA-co-APMA-D)-b-PEG is not visible in the DSC graph shown in SI-Figure 5. As there is no visible peak within the range of 30 to 150°C, it can be concluded that the melting point for this polymer lies outside this range.

The PEGylated block copolymer shown in SI-Figure 6 (D) showed a small onset of degradation between 20°C and 150°C with around 12% weight loss. % Weight loss showed a larger decrease at 151.88°C and fully degraded around 458.14°C. The PEGylated block copolymer degraded over a larger range of temperatures at a slower rate than the HPMA-APMA monomers.

3.4 Drug Loading of HMPA copolymers

The polymers were synthesised at varied ratios of substituted APMA monomers, which impacted their solubility, seen in Table 4. The HPMA copolymer solubility tends to decrease as the presence of the lipophilic pendant group increases, with as little as 1% cholesteryl inclusion in the copolymer being sufficient to render the polymer insoluble. Therefore, only those polymers that exhibited water solubility were taken forward to the drug loading study. Figure 5A shows the maximum drug loading of propofol within the HPMA copolymer formulations. Based on literature precedence, it is expected that the drug is residing inside the lipophilic core of the core-shell aggregate formed in aqueous environments [2]. The maximum amount of propofol solubilised in P-0.25, C-0.25 and D-2 being up to 313-fold (31.3 $mgmL^{-1}$), 317-fold (31.7 $mgmL^{-1}$), and 347-fold (34.7 $mgmL^{-1}$), more than its aqueous solubility (0.1 $mgmL^{-1}$), respectively. Results from the propofol loading study with different APMA-R grafting ratios are presented in SI-Figure 7. SI-Figure 7A compares drug loading using varied palmitoyl grafting levels. The data showed solubilisation increased with increased polymer concentration and increased drug loading feed ratio. However, the highest propofol loading was observed with the 0.25 % palmitoyl polymer with less being incorporated with the 1% palmitoyl copolymer. This was unexpected, as at a higher level of palmitoyl content, greater hydrophobicity exists which was expected to give rise to greater solubility. It could be that the long chains were not enough to stabilise greater loading influx and, hence, the 0.25% grafted nano-aggregates were more efficient. A similar trend was observed in the HPMA-co-APMA-D study, whereby increasing polymer concentration and loading feed ratio resulted in greater solubility. The data also showed that increasing the presence of APMA-D in the HPMA-co-APMA-D also increased drug encapsulation and, hence, solubilisation (SI-Figure 7B). At 2 % molar grafting the greatest propofol encapsulation was observed with 34.66 $mgmL^{-1}$ solubilised (1:10 polymer:drug ratio). Solubilisation of propofol using the only cholesteryl level which delivered a soluble polymer (C-0.25) followed the trend observed in the polymers grafted with palmitoyl and dansyl, whereby the highest level of drug solubilisation was achieved at 6 $mgmL^{-1}$ and 1:10 polymer:drug initial feed ratio, resulting in a 317-fold increase compared with aqueous solubility (SI-Figure 7C).

The ability of the HPMA-co-APMA-R copolymers to solubilise other drug compounds and act as effective solubility enhancers was investigated using griseofulvin and prednisolone. The maximum solubilisation of griseofulvin in the polymers is shown in Figure 5B. The data shows that the polymers were indeed capable of enhancing the aqueous solubility of griseofulvin, with the palmitoyl pendant being most effective, showing a 693-fold increase (20.8 $mgmL^{-1}$) from intrinsic solubility (0.03 $mgmL^{-1}$) as compared to a 400-fold enhancement with the dansyl modified polymer (12.0 $mgmL^{-1}$) and a 340-fold enhancement with the cholesteryl derivative (10.2 $mgmL^{-1}$). SI-Figure 8A shows the concentration of griseofulvin encapsulated inside the HPMA-co-APMA-P polymer, where increased griseofulvin encapsulation was observed at 1:10 polymer:drug initial feed ratio at 6 $mgmL^{-1}$ (20.8 $mgmL^{-1}$) of P-0.25, than for P-1 at the same ratio (9.2 $mgmL^{-1}$), which is in agreement with the propofol data. SI-Figures 8B shows the drug encapsulation data for the dansyl polymer derivatives. HPMA-co-APMA-D self-assemblies showed that encapsulation improved with increasing grafting ratio, and greater solubility was achieved with 2% dansyl. The trend was not so clear with the cholesteryl grafted polymer (SI-Figure 8C); here, the greatest loading was observed at 3 $mgmL^{-1}$.

Figure 5C indicated similar maximum prednisolone encapsulation abilities of the polymer derivatives. Here, the dansyl polymer resulted in the greatest solubilisation with a 65.5-fold (13.1 $mgmL^{-1}$) increase from aqueous solubility (0.2 $mgmL^{-1}$). Similar trends were observed for prednisolone encapsulation inside the P-0.25 and C-0.25 polymers with a 55-fold (11.0 $mgmL^{-1}$) and 50-fold (9.9 $mgmL^{-1}$) solubilisation enhancement observed, respectively (SI-Figure 9).

Particle size distribution of the optimal HPMA formulations (as observed from SI-Figures 7-9) can be seen in Table 4. The data indicates that size of the self-assemblies after encapsulation of the model drugs is varied. This variance in size was influenced by the molecular weight and presumably the stereochemistry of the drug molecules being loaded. As expected, the empty nano-aggregates possessed particle sizes in the nanoscale which were consistently smaller than those which had drugs encapsulated within. Particle size of P-0.25, C-0.25, and D-2 without drug was found to be 140 nm, 100 nm and 200 nm, respectively, with relatively high polydispersity indexes (PDI) of 0.7, 0.7 and 0.5, respectively. After drug loading the sizes increased, with prednisolone expanding the aggregates to 5000 nm; however, this measurement is out with the range (2-1000 nm) of the instrument used so may not be very accurate. Nevertheless, a large size increase was noted.

3.5 *In vitro* drug release from HMPA copolymers

The effect of temperature increases on the drug release profile of the thermally active polymer formulations was investigated at 5 ºC, 30 ºC, 40 ºC and 50 ºC. The data for propofol release from those formulations which exhibited highest drug loading for each pendant group are shown in Figure 6A-C. The data indicated that the HPMA-co-APMA-R copolymers did not release drugs more rapidly at elevated temperatures. Indeed the opposite was true, with the drug appearing to be retained within the polymer aggregate at the highest temperature of 50 ºC. Furthermore, varying the pH of the outer solution did not affect the dissolution profiles (data not shown). To combat this, the polymers were block copolymerised with PEG in order to alter the release characteristics.

3.6 Drug loading and *in vitro* drug release from PEGylated HPMA block copolymer

PEGylation was carried out with the dansyl (2%) copolymer at a 10:90 monomer ratio respectively, which showed optimal loading potential for both propofol and prednisolone, but also because of the fluorescent nature of dansyl, which could be exploited in follow on studies

should the data be favourable. The data showed that the solubilisation ability of (D-2)-b-(PEG) with propofol and prednisolone was decreased with the addition of PEG compared to the un-PEGylated polymer (Figure 5D-F). This is likely a consequence of the inclusion of PEG into the polymer structure, whereby the hydrophilic properties of the PEG shifts the hydrophilic-hydrophobic balance of the amphiphilic copolymer. Interestingly, the solubilisation of griseofulvin did not appear to be affected by this, perhaps because the limiting factor in griseofulvin solubilisation may be its steric hindrance at high concentrations, which still dominated with the PEGylated polymer. The (D-2)-b-(PEG) was capable of increasing drug concentrations compared to the aqueous solubility up to 142-fold (14.2 $mgmL^{-1}$) for propofol, 467-fold for griseofulvin (14.0 $mgmL^{-1}$) and 41-fold for prednisolone (8.2 $mgmL^{-1}$), respectively. Interestingly, the addition of PEG into the polymer structure did not have any significant impact on particle size (Table 4), except in the prednisolone formulation where the vast size expansion experienced in the unPEGylated polymer was not observed.

After introduction of PEG, the drug release profile changed dramatically (Figure 6D). Instead of observing a relatively slow and steady release over the study period, the drugs were released much more rapidly. For propofol, 70% (19.9 mg) of drug had been released after 24 h at 40 °C, compared to 30% (8.5 mg) in the un-PEGylated counterpart. Both griseofulvin and prednisolone were 100% (28 mg and 16.4 mg, respectively) released at 50 °C after only 4 h, compared with only 20% in the polymer without PEG. Interestingly, in the propofol study more drug was released at 40 °C than at 50 °C, the reason for which is unclear; perhaps the polymer shrinkage occurs more rapidly at this temperature resulting in a tighter core, thus restricting drug release. This observation was not evident in the prednisolone or griseofulvin studies.

4. Discussion

The chemical analysis confirmed that the pendant groups were successfully grafted onto the APMA monomers. The choice of pendant group was based on the literature. Choudhari *et al.*, reported the acylation of low molecular weight chitosan using palmitoyl chloride at the primary amine [17]. This resulted in a large increase in the ability of the micro emulsion to solubilise drug compounds. They reported drug loading of 5-fluorouricil increasing from 13.8 ± 0.95% up to 30.2 ± 1.9%. Additionally, 80 ± 2.08% of drug was released within 10 h whilst 52.3 ± 2.14% was released over 24 h, resulting in a more controlled system after inclusion of the palmitoyl moiety [17]. Additionally, Thompson *et al.* reported the formation of poly(allylamine) (PAA) graft amphiphiles via modification of random grafting of palmitoyl pendants onto the homopolymer backbone, before quaternisation. Here they studied the ability of the spontaneously formed nano-aggregates to complex insulin [10]. It was shown that all of the polymers were less cytotoxic after modification than the parent cationic PAA homopolymer, whilst high levels of insulin complexation efficiency was observed (up to 93%) [10].

When dansyl and cholesteryl pendants have been incorporated into an amphiphilic polymer, their resultant nano-aggregates have been shown to act as universal drug solubilizers [12]. The dansyl moiety has the added benefit of its intrinsic fluorescent nature. Fluorescent delivery systems are very desirable due to their ability to be tracked *in vivo*, allowing a better understanding of their fate. Nanoparticles, which possess inherent fluorescence, are also a potential alternative to the traditional molecular fluorophores in applications such as cell labelling or sensing [18]. Cholesterol and its derivatives are naturally occurring molecules, which can possess either amphiphilic or lipophilic nature, based on their molecular structures [19]. Cholesterol possesses the ability to easily cross cell membranes, and has thus been explored in multiple delivery vehicles [20]. Lee and colleagues reported large paclitaxel

encapsulation efficiency of 92% using the cationic micelles of amphiphilic poly{(*N*-methyldietheneamine sebacate)-co-[(cholesteryl oxocarbonylamido ethyl) methyl bis(ethylene)ammonium]} (PMDS) [21]. The micelles reported had been conjugated to poly (ethylene glycol) (PEG) with varied levels of cholesterol grafting in order to enhance stability of the micelle/DNA complexes formed in the blood. Yong and colleagues reported that PMDS and PEG-PMDS without cholesterol in their structure were not capable of forming form stable micelles; instead, aggregation into large clusters was observed [22]. Our study agreed with the literature, showing that all three pendant groups were hydrophobic enough to result in self-assembly formation in aqueous environments. Also in agreement with other studies, a high level of drug solubility enhancement was observed, whereby all three drug molecules tested (propofol, prednisolone and griseofulvin) were solubilised within the core of the nano-assemblies, despite their differences in lipophilicity, molecular weight and structural architecture.

Free radical polymerization consists of initiation, propagation and termination steps. The termination step can proceed via route A or route B (Figure 7). In this work, the ^{1}H NMR spectrum indicated the presence of peaks at 5.4-5.7 ppm, which can be attributed to olefinic protons. These arise from hydrogen atoms in the alkene groups, indicating that the disproportionation reaction had proceeded via route A [23]. In general, at increased copolymerisation ratio, the polymers were capable of greater levels of solubilisation of the lipophilic model drug compounds. However, at high levels, this further increase in the hydrophobicity can result in large aggregate formation and these are likely removed in the filtration step, thus impacting on the observed drug loading ability. We observed that drug encapsulation was increased as the initial polymer:drug mass loading ratios were increased, although this was not observed in all cases. When the drug encapsulation increases, this results in the hydrophobic interaction between adjacent drug molecules increasing rather than that between drug and copolymers [24].

Based on the observations, HPMA-co-APMA-D (D=2%) seemed to be the best overall polymer for enhancing the solubilities of the model hydrophobic drugs, as shown in Figure 5. The drug is presumed to be located within the lipophilic core of the core-shell aggregate formed [2]. Subsequently, this polymer was further polymerised with PEG in order to optimise its thermally active nature to suit our application. The literature suggests that PEGylation results in a better prolonged control over drug diffusion rate. Block copolymers of poly(ethylene glycol) with poly(trimethylene carbonate) (PEG−PTMC) have been shown to undergo reverse gelation at temperatures between 20 to 75 °C. This transition temperature for physical change can be tailored for our application by altering molecular weight, polymer concentration, or polymer composition [25]. The HPLC data showed that HPMA-co-APMA-D-b-PEG was not as effective at solubilising the lipophilic drug molecules compared to its unPEGylated counterpart. This is due to the hydrophilic properties of the PEG, which shifts the hydrophobic-hydrophilic balance of the overall system, resulting in a reduced ability to solubilise lipophilic drug payloads. However, before PEGylation the cargo release occurred more rapidly and at lower temperatures but with less control. In agreement with the literature, after PEGylation more control over the release rate and need for elevated temperatures in order for cargo release to occur was observed. Therefore, the PEG was deemed an essential component of these systems moving forward. PEG also provides additional protection from premature immune system capture and anti-fouling properties upon long-term systemic circulation, hence, its benefits are numerous.

Propofol, griseofulvin and prednisolone have been reported as model hydrophobic drugs in

multiple solubilisation studies. This is due to their low cost, high lipophilicity, varied molecular weight and stereochemistry, and problematic experiences on or after administration. Recently, Hoskins *et al.*, reported the potential of calix[4]resorcinarenes which had been sulfonated for drug solubilisation. They reported enhanced propofol and griseofulvin solubility in aqueous solution compared to their intrinsic values. They found that increasing the length of n-alkyl chains on the lower rim from n= 4 to 7 carbons led to the ability to solubilise propofol and griseofulvin up to 3 $mgmL^{-1}$ and 8 $mgmL^{-1}$, respectively [26]. Chitosan- based amphiphilic polymers (Mw < 20 kDa) which form nano-aggregates in aqueous media were reported by Qu *et al* [27]. They showed that after formulation with their nano-aggregates, enhancement of both solubility and bioavailability of propofol and prednisolone was observed [27]. The micellar structures formed were capable of solubilisation of up to 4.43 $mgmL^{-1}$ and 1 $mgmL^{-1}$, respectively [27]. Excitingly, our data shows even better solubilisation compared to previous studies with greater compound internalisation and, hence, solubilisation. Therefore, in order to achieve similar solubilities as other systems, or therapeutic dosages of these specific compounds, the amount of polymer or drug feed ratio could be reduced, making the technology more efficient. Additionally, this also speculatively gives promise as a candidate solubilising agent which may be used for those more bulky, stubborn 'brick dust' like drugs which have either been formulated in the past in oily viscous injectables or totally disregarded because of their high logP value. Such compounds are found in drug discovery programmes for cancer, in particular. Thermo-responsive delivery of compounds is desired particularly in cancer nanomedicine where control over potent compound delivery is essential. Temperature activation has been extensively studied for precision drug release from various delivery systems [28-30]. Thermally active polymers experience a rapid change in physical properties as a response to change or fluctuation in the environmental temperature; this renders them exciting new platforms as candidates for the loading and carriage of potent anticancer compounds. Wadajkar *et al.* reported novel magnetic core-shell particles (MBCSP) consisting of a thermally active shell of poly(*N*-isopropylacrylamide-acrylamide-allylamine) with a poly (lactic-co-glycolic acid) (PLGA) core for the targeting and treatment of skin cancer [31]. They showed that (MBCSP) released their cargo rapidly at elevated temperature [31]. In our study, propofol release from the formulations indicated that upon increase of the surrounding temperature a corresponding decrease in drug release from the HPMA-co-APMA-R copolymers was observed. We believe that at elevated temperatures, the polymer was contracting around the drug and hindering its release (Figures 6A-C). The conjugation of the APMA-R residues to the HPMA in the copolymerisation can alter the transition temperature, or even make it disappear. Such ability is due to a shift in the change in hydrophilic/hydrophobic balance [32]. Therefore, by inclusion of a hydrophilic PEG block into the HPMA-co-APMA-R structure, the problem can be redressed. The HPMA-co-APMA-D-b-PEG release data confirms this theory as a temperature-controlled release was observed. Therefore, we are cautiously optimistic that the nanotechnologies developed could have benefit in cancer therapeutics. As the studies reported here are only showing *in vitro* drug release, further work is required in order to extend investigations into their mechanisms of action and cytotoxicities, both *in vitro* and *in vivo*, before their true potential could be realised. Based on this proof of concept study, looking at multiple variations of polymer type, copolymer ratio, and drug loading ratios we can suggest that our optimal system, based on the loading of the 2% danysl modified polymers, and that PEGylation of these polymers was essential in order to possess the triggered drug release desired. Further work is ongoing in our laboratories in order to develop an inbuilt switch, which can be externally triggered to initiate the heat-release of cargo demonstrated *in vitro* in this work.

5. Conclusion

The HPMA-APMA derivatives developed were capable of enhancing drug solubility. However, without the addition of PEG into the polymer structure the desired thermo-responsive release was not achieved. Nevertheless, after inclusion of PEG the polymers exhibited a thermo-responsivity at elevated temperatures, whereby the aggregate core was disrupted due to polymer precipitation and shrinkage, forcing expulsion of drug into the surrounding media. Thus, this approach holds promise for future delivery of compounds where precision control over release properties is required. Further work is required before the potential is realised, including more extensive characterisation of the aggregates and biological investigation into the potential toxicity of the systems. However, the data presented does set an exciting baseline for future work.

6. Acknowledgements
We would like to thank the Iraqi Ministry of Higher Education and Scientific Research (MOHSER) who funded this work.

7. Author Contributions
AA and EM carried out the laboratory work under the supervision of CH, DL and AC. CH wrote the manuscript. All authors approved the manuscript before submission.

8. Conflict of Interest
The authors would like to state there is no conflict of interest.

9. References

1. Taskeen, S., Pradeep, K., Yahya C.E., Viness, P., 2020. Hybrid Thermo-Responsive Polymer Systems and Their Biomedical Applications. Frontier. Mater. 7, 73.
2. Bobde, Y., Biswas, S., Ghosh, B., 2020. Current trends in the development of HPMA-based block copolymeric nanoparticles for their application in drug delivery. Eur. Polym. J. 139, 110018.
3. Talelli, M., Rijcken, C., Nostrum, C., Storm, G., Hennink, W., 2010. Micelles based on HPMA copolymers. Adv. Drug Deliver. Rev. 62, 231-239.
4. Das, S.S, Bharadwaj, P., Bilal, M., Barani, M., Rahdar, A., Taboada, P., Bungau, S., Kyzas, G.Z., 2020 Polymers. 12, 1397.
5. Alsuraifi, A., Curtis, A., Lamprou, D.A., Hoskins, C., 2018, Stimuli Responsive Polymeric Systems for Cancer Therapy. Pharmaceutics. 10, 136.
6. Ellah, N.A., Taylor, L., Troja, W., Owens, K., Ayres, N., Pauletti, G., Jones, H., 2015. Development of non-viral, trophoblast specific gene delivery for placental therapy. PLoS ONE. 10, 1-13.
7. Johnson, R.N., Chu, D.S.H., Shi, J., Schellinger, J.G., Carlson, P.M., Pun, S.H., 2011. HPMA-oligolysine copolymers for gene delivery: optimization of peptide length and polymer molecular weight. J. Control. Release. 155, 303-311.
8. Mendonça, P.V., Serra, A.C., Popov, A.V., Guliashvili, T., Coelho, J.F.J., 2014. Efficient RAFT polymerization of N-(3- aminopropyl)methacrylamide hydrochloride using unprotected ‘‘clickable’’ chain transfer agents. React. Funct. Polym. 81, 1-7.
9. Chu, D.S., Sellers, D.L., Bocek, M.J., Fischedick, A.E., Horner, P.J., Pun, S.H., 2015. MMP9-sensitive polymers mediate environmentally-responsive bivalirudin release and thrombin inhibition. Biomat.Sci. 3, 41-45.
10. Thompson, C.J., Tetley, L., Uchegbu, I.F., Cheng, W.P., 2009. The complexation between novel comb shaped amphiphilic polyallylamine and insulin-towards oral insulin delivery. Int. J. Pharm. 376, 46-55.
11. Hoskins, C., Kong Thoo Lin, P., Tetley, L., Cheng, W.P., 2012. The use of nano

polymeric self-assemblies based on novel amphiphilic polymers for oral hydrophobic drug delivery. Pharm. Res. 29,782-794.

12. Hoskins, C., Kong Thoo Lin, P., Tetley, L., Cheng, W.P., 2012. Novel fluorescent amphiphilic poly(allylamine) and their supramacromolecular self-assemblies in aqueous media. Polym. Adv. Technol. 23, 71-719.
13. Hoskins, C., Ouaissi, M., Costa, S.L., Cheng, W.P., Loureirio, I., Mas, E., Lombardo, D., Cordeiro, A., Ouaissi, A., Kong Thoo Lin, P., 2010. *In vitro* and *in vivo* anticancer activity of a novel nano- sized formulation based on self-assembling polymers against pancreatic cancer. Pharm. Res. 27, 2694-703.
14. Wanga, Y., Lia, J., Chena, Y., Oupický, D., 2015. Balancing polymer hydrophobicity for ligand presentation and siRNA delivery in dual function CXCR4 inhibiting polyplexes. Biomat. Sci. 3, 1114- 1123.
15. Zheng, S., Xie, Y., Li, Y., Li, L., Tian, N., Zhu, W., Yan, G., Wu, C., Hu, H., 2014. Development of high drug- loading nanomicelles targeting steroids to the brain. Int. J. Nanomed. 9, 55-66.
16. Yu, F., Li, J., Sleightholm, R.L., Oupický, D., 2016, Polymeric chloroquine as an inhibitor of cancer cell migration and experimental lung metassis. J. Control. Release. 244, 347-356.
17. Choudhari, Y.M, Detane, S.V., Kulthe, S.S., Godhani, C.C., Inamdar, N.N., Shirolikar, S.M., Borde, L.C., Mourya, V.K., 2012. Low molecular weight palmitoyl chitosan: Synthesis, characterization and nanoparticle preparation. Adv. Mater. Lett. 3, 487-492.
18. Ouadahi, K., Sbargoud, K., Allard, E., and Larpent, C., 2012. FRET-mediated pH-responsive dual fluorescent nanoparticles prepared via click chemistry. Nanoscale. 4, 727-732.
19. Zhou, Y., Briand, V.A., Sharma, N., Ahn, S.k., Kasi, R.M., 2009. Polymers comprising cholesterol: synthesis, self-assembly, and applications. Materials. 2, 636-660.
20. Sevimli, S., Inci, F., Zareie, H.M., Bulmus, V., 2012. Well-defined cholesterol polymers with pH-controlled membrane switching activity. Biomacromol. 13, 3064-3075.
21. Lee, A.L.Z., Wang, Y., Pervaiz, S., Fan, W., Yang, Y.Y., 2011. Synergistic anticancer effects achieved by co-delivery of TRAIL and paclitaxel using cationic polymeric micelles. Macromol. Biosci. 11, 296-307.
22. Yong, W., Kea, C-Y., Beha, C.W., Liua, S-Q, Goh, S-H., Yang, Y.Y., 2007. The self-assembly of biodegradable cationic polymer micelles as vectors for gene transfection. Biomaterials. 28, 5358-5368.
23. Hatada, K., Kitayama, T., Masuda, E., 1986. Studies on the radical polymerization methyacrylate in bulk and benezene using totally deuterated monomer technique. Polym. J., 18, 395-402.
24. Ding, M., Zhou, L., Fu, X., Tan, H., Li, J., Fu, Q., 2010. Biodegradable gemini multiblock poly(ε-caprolactone urethanes toward controllable micellization. Soft Matter. 6, 2087-2092.
25. Kim, S.Y., Kim, H.J., Lee, K.E., Han, S.S., Sohn, Y.S., Jeong, B., 2007. Reverse thermal gelling PEG−PTMC diblock copolymer aqueous solution. Macromolecules. 40, 5519-5525.
26. Hoskins, C., Papachristou, A., Ho, T.M.H., Hine, J., Curtis, A.D.M., 2016. Investigation into drug solubilisation potential of sulfonated calix[4]resorcinarenes. J. Nanomed. Nanotechnol. 7, 370-377.
27. Qu, X., Khutoryanskiy, V.V., Stewart, A., Rahman, S., Papahadjopoulos-Sternberg, B., Dufes, C., McCarthy, D., Wilson, C.G., Lyons, R., Carter, K.C., Schatzlein, A., Uchegbu, I.F., 2006. Carbohydrate-based micelle clusters which enhance hydrophobic

drug bioavailability by up to 1 order of magnitude. Biomacromolecules. 7, 3452-3459.
28. Zhu, Y., Zeng, Q., Zhang, Q., Li, K., Shi, X., Liang F., Han., D., 2020. Temperature/near-infrared light-responsive conductive hydrogels for controlled drug release and real-time monitoring. Nanoscale. 12, 8679-8686.
29. Abdo, G.G., Zagho, M.M., Khalil, A., 2020. Recent advances in stimuli-responsive drug release and targeting concepts using mesoporous silica nanoparticles. Emergent Mater. 3, 407–425.
30. Qiao, Y., Wan, J., Zhou, L., Ma. W., Yang. Y., Luo. W., Yu. Z., Wang. H., 2019. Stimuli-responsive nanotherapeutics for precision drug delivery and cancer therapy. WIREs Nanomed Nanobiotechnol. 11, e1527.
31. Wadajkar, A.S., Bhavsar, Z., Ko, C-Y., Koppolu, B., Cui, W., Tang, L., Nguyen, K.T., 2012. Multifunctional particles for melanoma-targeted drug delivery. Acta Biomaterialia. 8, 2996-3004.
32. Gandhi, A., Paul, A., Sen, S.O. Sen, K.K., 2015. Studies on thermoresponsive polymers: phase phase behaviour, drug delivery and biomedical applications, Asian J. Pharm. Sci. 10, 99-107.

Figures

Figure 1. Schematic representation of HPMA-APMA derivatives for thermo-responsive drug delivery.

Figure 2. Polymerisation route for poly(HPMA-APMA-R) copolymers.

Figure 3. Block copolymerisation route for the inclusion of PEG forming (HPMA-co-APMA-R)-b-PEG.

Figure 4. ^{1}H NMR spectra of HPMA-AMPA polymers A) HPMA-co-AMPA-P, B) HMPA-co-AMPA-D, C) HPMA-co-AMPA-C and D) HPMA-co-APMA-D-b-PEG. All modified monomers analysed in $CDCl_3$ carried out using 300MHz NMR at 25 °C.

Figure 5. Drug loading data for A-C optimal formulations and D-F effect of loading concentration and feed ratio of HMPA-co-APMA-D-b-PEG on A) propofol, B) griseofulvin and C) prednisolone (n=3 ± SD).

Figure 6. *In vitro* drug release data for 1) propofol, 2) griseofulvin and 3) prednisolone from A) HMPA-co-APMA-P B)HMPA-co-APMA-D C) HMPA-co-APMA-C and D) HMPA-co-APMA-D-b-PEG amphiphiles at 5°C,30°C,40°C and 50°C in water (n=3 ± SD).

Figure 7. Disproportionation termination routes.

Tables

Table 1. Monomer feed ratio of poly(HPMA-APMA-R) copolymers.

Table 2. Physical properties of the modified monomers.

Table 3. Effect of grafting hydrophobic pendant groups to the copolymers solubility.

Table 4. Photon correlation spectrometry of optimal formulations (n=3, ± SD).

Tables

Table 1

Copolymerisation ratio % pendant modification	Mole fraction of HPMA, M1	Mole fraction of APMA-R, M2	Monomer feeding ratio (APMA-R / HPMA) per gram			
			APMA-Palmitoyl (APMA-P)	APMA-Dansyl (APMA-D)	APMA-Cholesteryl (APMA-C)	AIBN per gram
0.25	99.75	0.25	0.0035/0.5000	0.0033/0.5000	0.0049/0.5000	0.0055
1	99	1	0.0236/0.8448	0.0224/0.8448	0.0340/0.8448	0.0055
2	98	2	0.0476/0.8448	0.0453/0.8448	0.0669/0.8448	0.0055
5	95	5	0.1202/0.8202	0.1144/0.8202	0.1690/0.8202	0.0055
10	90	10	0.2380/0.7770	0.2264/0.7770	0.3346/0.7770	0.0055

Table 2

Modified monomer	Molecular formula	Molecular weight	Appearance	Physical state	Melting Point °C	Rf	Yield %
APMA-Palmitoyl (APMA-P)	$C_{16}H_{44}N_2O_2$	394.63	White	Powder	91.5	0.39	79
APMA-Dansyl (APMA-D)	$C_{19}H_{25}N_3O_3S$	375.48	Yellow	Thick liquid	-----	0.66	65
APMA-Cholesteryl (APMA-C)	$C_{35}H_{58}N_2O_3$	554.84	White	Powder	154.5	0.74	75

Table 3

Copolymerization Ratio % pendant modification	**HPMA-co-APMA-P /Copolymer Code**	**HPMA-co-APMA-D / Copolymer Code**	**HPMA-co-APMA-C / Copolymer Code**
0.25	✓ P-0.25	✓ D-0.25	✓ C-0.25
1	✓ P-1	✓ D-1	-
2	-	✓ D-2	-
5	-	-	-
10	-	-	-

Table 4

Copolymer	Formulation Size (nm)				Formulation PDI			
	Alone	Propofol	Griseofulvin	Prednisolone	Alone	Propofol	Griseofulvin	Prednisolone
HPMA-co-APMA-P-0.25	140 ± 20	900 ± 9	200 ± 7	1100 ± 200	0.7 ± 0.2	0.3 ± 0.0	0.4 ± 0.0	0.8 ± 0.0
HPMA-co-APMA-C-0.25	100 ± 10	500 ± 20	300 ± 10	600 ± 8	0.7 ± 0.2	0.4 ± 0.0	0.2 ± 0.0	0.3 ± 0.0
HPMA-co-APMA-D2	200 ± 10	3300 ± 90	200 ± 10	5000 ± 400	0.5 ± 0.1	0.3 ± 0.1	0.8 ± 0.3	0.7 ± 0.1
HPMA-co-APMA-b-D2-PEG	200 ± 3	1500 ± 100	200 ± 40	900 ± 100	0.4 ± 0.0	0.4 ± 0.0	0.7 ± 0.1	0.8 ± 0.1

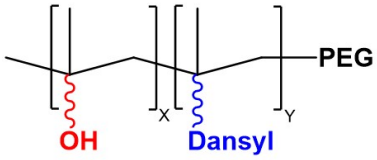

HPMA-co-APMA-D
D = Dansyl

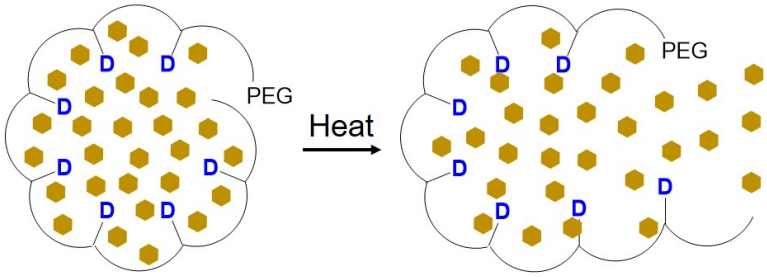

Figures

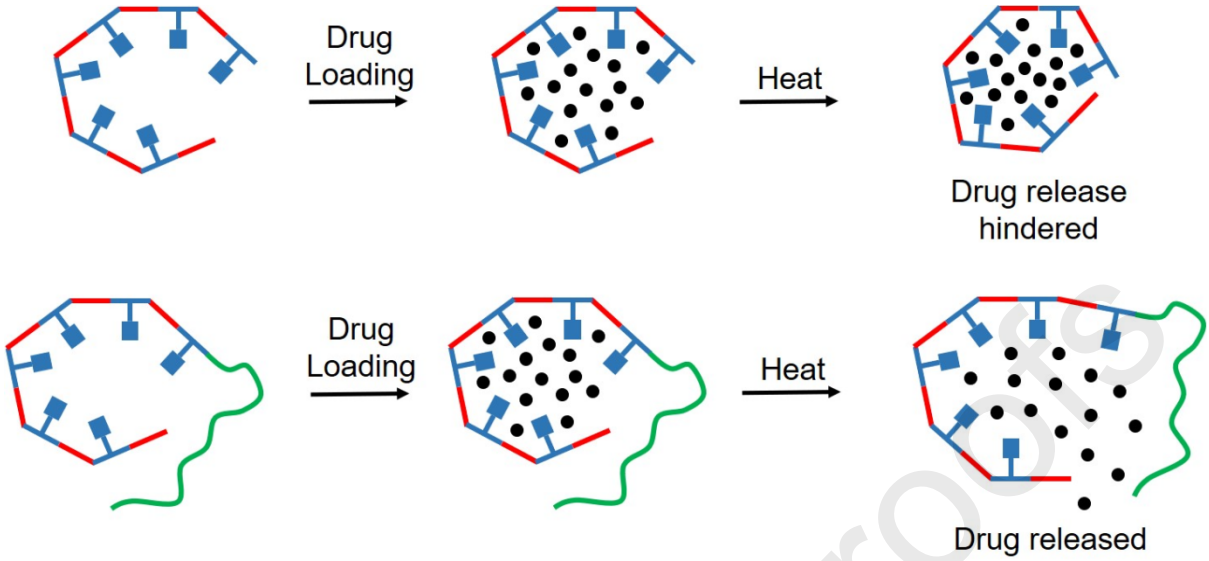

Figure. 1

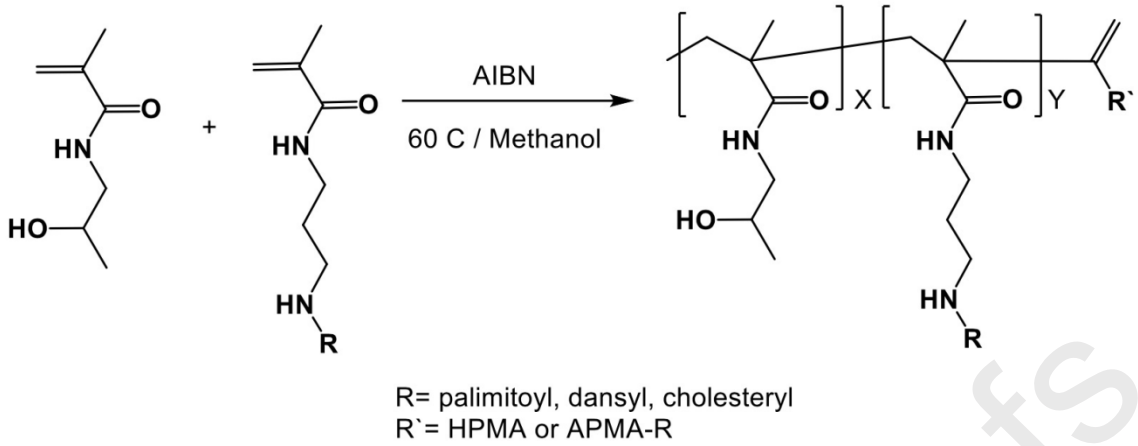

Figure. 2

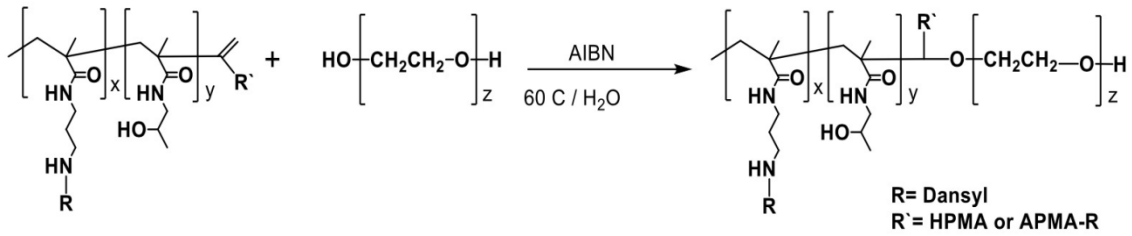

Figure. 3

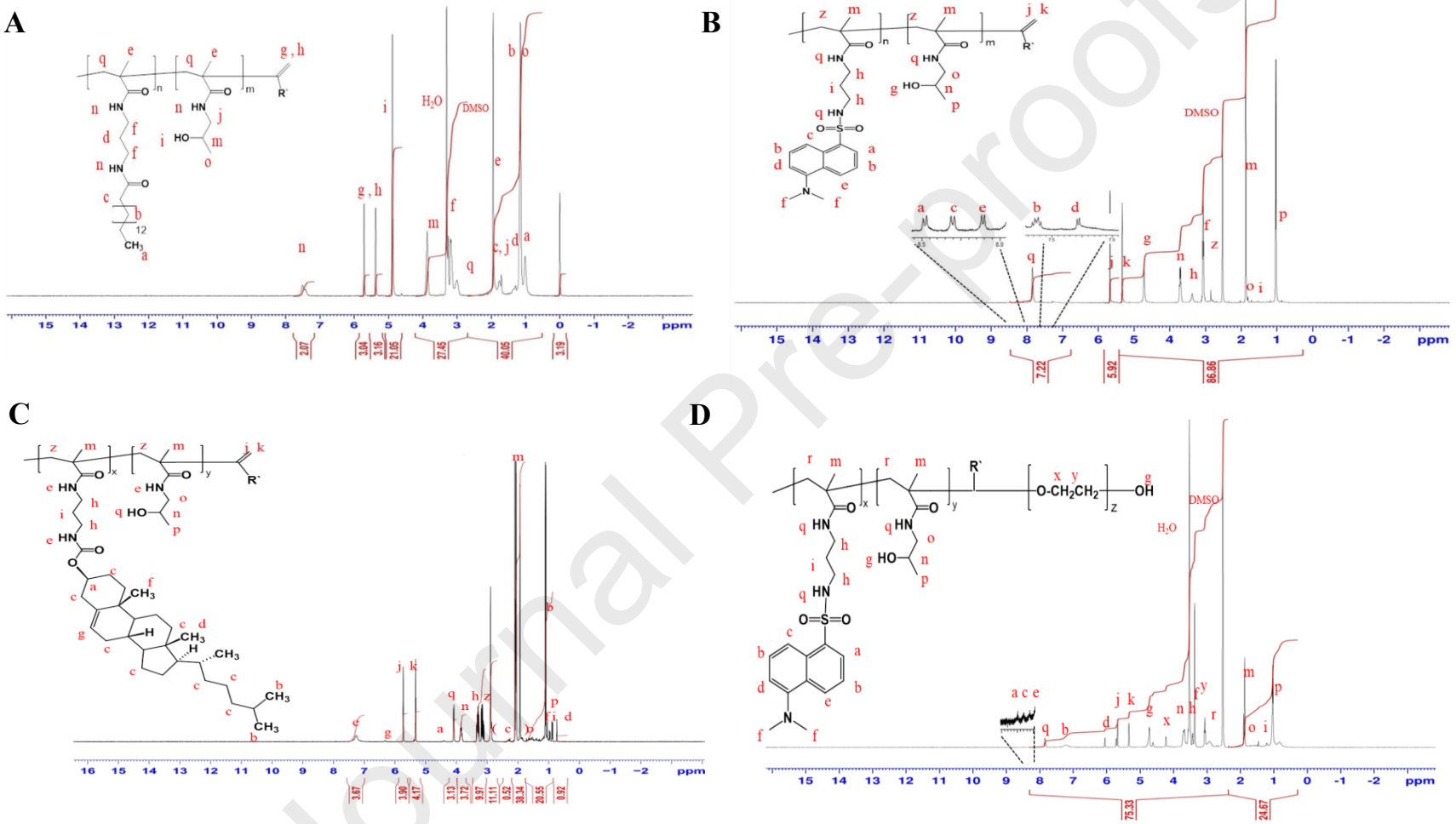

Figure. 4

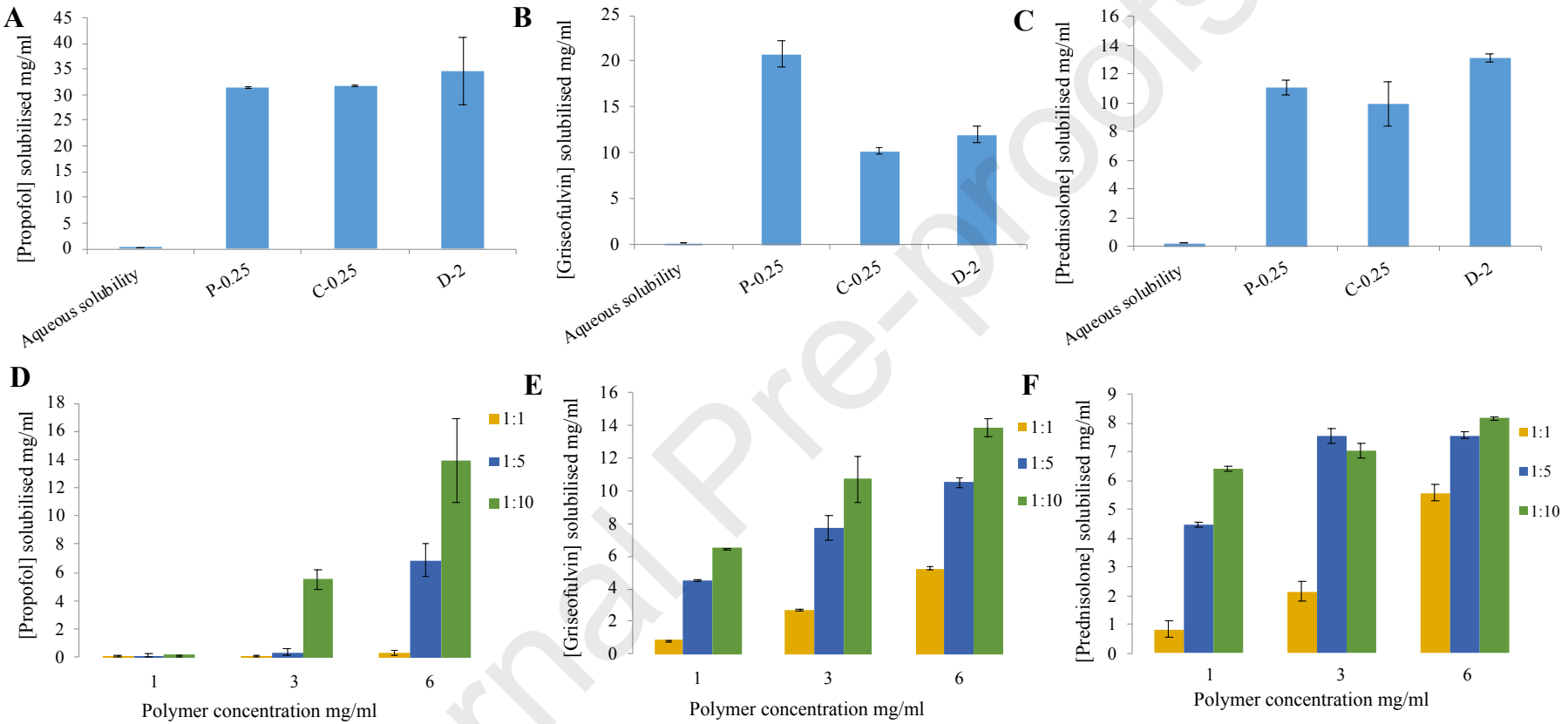

Figure. 5

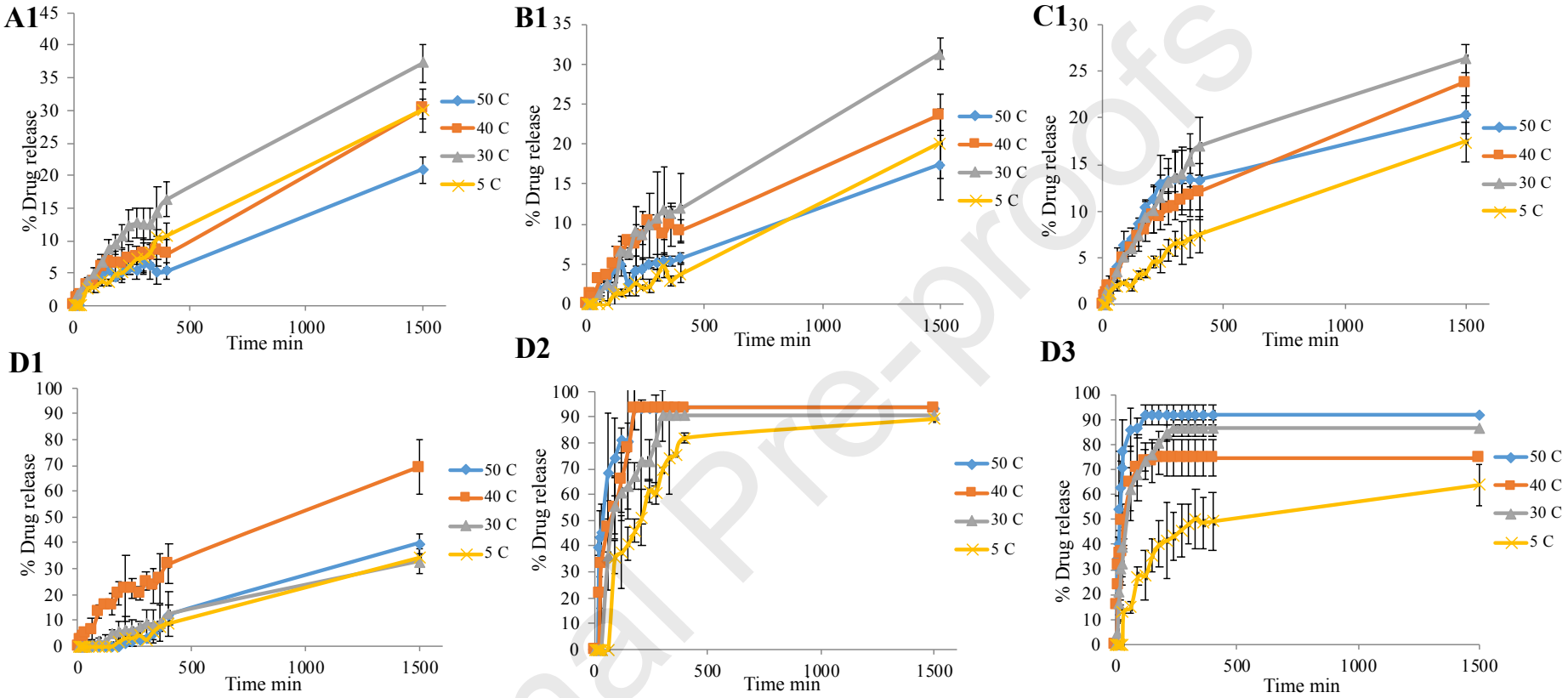

Figure. 6

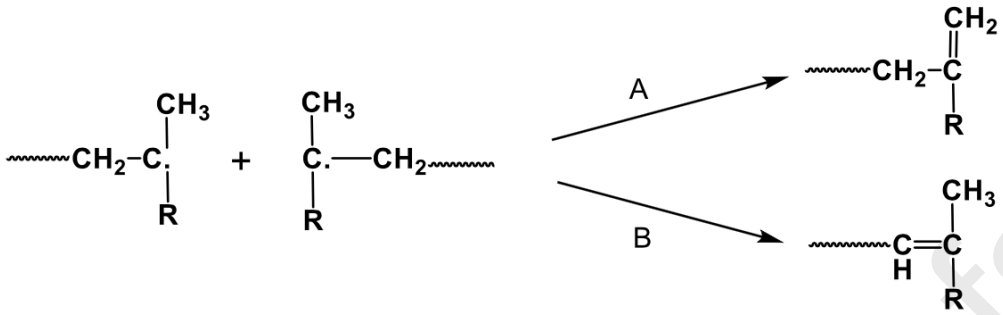

Figure. 7

Declaration of interests

☒ The authors declare that they have no known competing financial interests or personal relationships that could have appeared to influence the work reported in this paper.

☐The authors declare the following financial interests/personal relationships which may be considered as potential competing interests: